High-power lithium batteries from functionalized carbon-nanotube electrodes

Seung Woo Lee[1†], Naoaki Yabuuchi[2†], Betar M. Gallant[2], Shuo Chen[2], Byeong-Su Kim[1], Paula T. Hammond[1] and Yang Shao-Horn[2,3★]

Energy storage devices that can deliver high powers have many applications, including hybrid vehicles and renewable energy. Much research has focused on increasing the power output of lithium batteries by reducing lithium-ion diffusion distances, but outputs remain far below those of electrochemical capacitors and below the levels required for many applications. Here, we report an alternative approach based on the redox reactions of functional groups on the surfaces of carbon nanotubes. Layer-by-layer techniques are used to assemble an electrode that consists of additive-free, densely packed and functionalized multiwalled carbon nanotubes. The electrode, which is several micrometres thick, can store lithium up to a reversible gravimetric capacity of $\sim$200 mA h $g_{electrode}^{-1}$ while also delivering 100 kW $kg_{electrode}^{-1}$ of power and providing lifetimes in excess of thousands of cycles, both of which are comparable to electrochemical capacitor electrodes. A device using the nanotube electrode as the positive electrode and lithium titanium oxide as a negative electrode had a gravimetric energy $\sim$5 times higher than conventional electrochemical capacitors and power delivery $\sim$10 times higher than conventional lithium-ion batteries.

A major challenge in the field of electrical energy storage is to bridge the performance gap between batteries and electrochemical capacitors by developing materials that can combine the advantages of both devices. Batteries exhibit high energy as a result of Faradaic reactions in the bulk of active particles, but are rate-limited. Electrochemical capacitors[1–3] can deliver high power at the cost of low energy storage by making use of surface ion adsorption (referred to as double-layer capacitance) and surface redox reactions (referred to as pseudo-capacitance). Lithium rechargeable batteries ($\sim$150 W h kg_{cell}^{-1} and $\sim$1 kW kg_{cell}^{-1}) therefore have higher gravimetric energy but lower power capability than electrochemical capacitors ($\sim$5 W h kg_{cell}^{-1} and $\sim$10 kW kg_{cell}^{-1})[1]. Energy and power versatility are crucial for hybrid applications[2]. For example, although conventional batteries have been used in light vehicles, hybrid platforms for heavy vehicles and machineries demand delivery of much higher currents, so higher energy and comparable power capability relative to electrochemical capacitors are needed to meet this demand[1,2].

Considerable research efforts have been focused on increasing the power characteristics of lithium rechargeable batteries by reducing the dimensions of lithium storage materials down to the nanometre scale[4–12], which would reduce the lithium diffusion time that accompanies the Faradaic reactions of active particles. However, nanostructured lithium storage electrodes[5,13] still have a lower power capability than electrochemical capacitor electrodes. On the other hand, researchers have shown that the gravimetric energy of electrochemical capacitors can be increased by using electrode materials with enhanced gravimetric capacitances (gravimetric charge storage per volt), which can be achieved through the use of carbon subnanometre pores for ion adsorption[1,14] or by taking advantage of the pseudocapacitance of nanostructured transition metal oxides[15–17]. The high cost of ruthenium-based oxides is prohibitive for many applications, and the cycling instability of manganese-based oxides[17–19] remains a major technical challenge.

A promising approach is to use the Faradaic reactions of surface functional groups on nanostructured carbon electrodes, which can store more energy than the double-layer capacitance on conventional capacitor electrodes[1] and also provide high power capability.

Here, we report the use of an entirely different class of electrodes for lithium storage, which are based on functionalized multiwalled carbon nanotubes (MWNTs) that include stable pseudo-capacitive functional groups, and are assembled using the layer-by-layer (LBL) technique[20]. These additive-free LBL-MWNT electrodes exhibit high gravimetric energy (200 W h $kg_{electrode}^{-1}$) delivered at an exceptionally high power of 100 kW $kg_{electrode}^{-1}$ in Li/LBL-MWNT cells when normalized to the single-electrode weight, with no loss observed after completing thousands of cycles. LBL-MWNT electrodes show significantly higher gravimetric energy not only over electrochemical capacitor electrodes, but also over high-power lithium battery electrodes, with gravimetric powers greater than $\sim$10 kW $kg_{electrode}^{-1}$. In addition, cells (analogous to asymmetric electrochemical capacitors) consisting of LBL-MWNTs and a lithiated $Li_4Ti_5O_{12}$ (LTO) negative electrode have comparable gravimetric energy to LTO/$LiNi_{0.5}Mn_{1.5}O_4$ cells[21] at low gravimetric power, but can also deliver much higher energy at higher power. Gravimetric energy and power at the cell level may be estimated by dividing these values based on LBL-MWNT weight by a factor of $\sim$5 (ref. 22). Furthermore, we show that the Faradaic reactions between the lithium ions and the surface functional groups on the MWNTs are responsible for the high gravimetric energy found in Li/LBL-MWNT and LTO/LBL-MWNT cells.

Physical characteristics of LBL-MWNT electrodes
Stable dispersions of negatively and positively charged MWNTs were obtained by functionalization of the exterior surfaces with carboxylic-acid (MWNT–COOH) and amine-containing (MWNT–NH_2) groups, respectively[23]. Uniform MWNT electrodes on glass

[1]Department of Chemical Engineering, Massachusetts Institute of Technology, Cambridge, Massachusetts 02139, USA, [2]Department of Mechanical Engineering, Massachusetts Institute of Technology, Cambridge, Massachusetts 02139, USA, [3]Department of Materials Science and Engineering, Massachusetts Institute of Technology, Cambridge, Massachusetts 02139, USA; [†]These authors contributed equally to this work. *e-mail: shaohorn@mit.edu
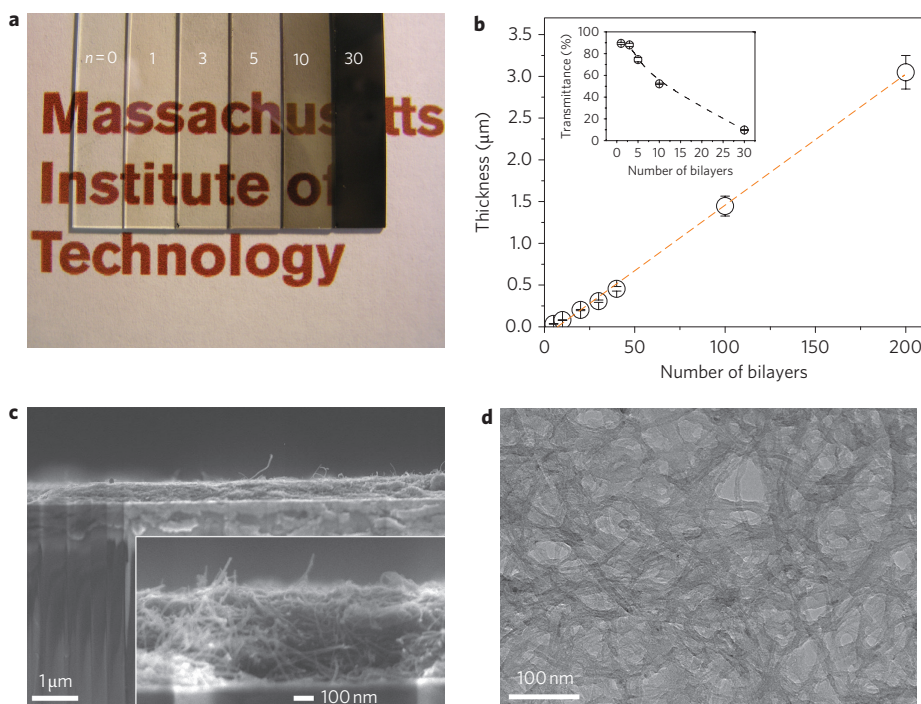
531

Figure 1 | Physical characteristics of LBL-MWNT electrodes. a, Digital image of representative MWNT electrodes on ITO-coated glass slides. The number on each image indicates the number of bilayers (n) in (MWNT–NH$_2$/MWNT–COOH)$_n$. **b**, Thickness of the LBL-MWNT electrodes as a function of the number of bilayers. A linear relationship is apparent for LBL-MWNT electrodes with thicknesses from 20 nm to 3 μm. Error bars show the standard deviation of the thickness, computed from three samples for each thickness. Transmittance measured at 550 nm as a function of the number of bilayers is shown in the inset. Error bars show the standard deviation of transmittance computed from three measurements. **c**, SEM cross-sectional image of an LBL-MWNT electrode on an ITO-coated glass slide after heat treatments. A higher-magnification image is shown in the inset, revealing that MWNTs are entangled in the direction perpendicular to the electrode surface. **d**, TEM image of an LBL-MWNT electrode slice, showing pore sizes of the order of ~20 nm.

coated with indium tin oxide (ITO) (Fig. 1a) were assembled by alternate adsorption of charged MWNTs[23]. Electrode thickness increases linearly with the number of positively and negatively charged layer pairs (bilayers), as shown in Fig. 1b. The transparency of the MWNT films decreased linearly with increasing thickness up to 0.3 μm (Fig. 1b). The films were then heat-treated sequentially at 150 °C in vacuum for 12 h, and at 300 °C in H$_2$ for 2 h to increase film mechanical stability and electrical conductivity[23]. Combined profilometry and quartz crystal microbalance measurements gave an electrode density of 0.83 g cm^{-3} (Supplementary Fig. S1) following the heat treatments, which is one of the highest densities reported for carbon nanotube electrodes[24,25]. Cross-sectional scanning electron microscope (SEM) images showed that the individual MWNTs were randomly distributed throughout the film thickness, and the MWNT films were uniform and conformal on the substrate (Fig. 1c). Moreover, the LBL-MWNT electrodes had an interconnected network of individual MWNTs (Fig. 1c, inset) with well-distributed pores of ~20 nm, as revealed by transmission electron microscopy (TEM) imaging of an LBL-MWNT electrode slice (Fig. 1d).

Role of surface functional groups on LBL-MWNT electrodes

X-ray photoemission spectroscopy (XPS) analysis of the LBL-MWNT electrodes after heat treatment revealed that significant amounts of oxygen-containing and nitrogen-containing surface functional groups remained on the nanotube surface. The atomic composition of a representative LBL-MWNT electrode was found to be 85.7% carbon, 10.6% oxygen and 3.7% nitrogen (C$_{0.86}$O$_{0.11}$N$_{0.04}$; Supplementary Table S1). The presence of two distinct peaks (531.7 ± 0.1 eV and 533.4 ± 0.1 eV) in the O 1s spectrum (Supplementary Fig. S2a) could be attributed to oxygen atoms in

the carbonyl groups[26,27] and various other oxygen groups (Supplementary Fig. S2c) bound to the edges[26,28] of the graphene sheets forming the MWNT sidewalls. High-resolution TEM images of functionalized MWNTs revealed that acid treatments roughened the exterior walls of the MWNTs (Supplementary Fig. S3), exposing carbon atoms on the edge sites. Edge carbon atoms are known to bind with oxygenated species more strongly than carbon atoms in the basal plane[29], which is in good agreement with the XPS finding that more oxygenated species are detected on LBL-MWNT electrodes than on pristine MWNTs. In addition, the chemical environment of the nitrogen atoms in the LBL-MWNT electrodes was mostly in the form of amide groups (Supplementary Fig. S2b), as indicated by the N 1s peak centred at 400.1 eV (ref. 30). Two small additional peaks in the N 1s spectrum suggest that some nitrogen atoms are pyridinic N-6 (ref. 30) (398.5 ± 0.1 eV) and tied in oxidized nitrogen-containing functional groups (402.3 eV)[30].

These surface functional groups can undergo Faradaic reactions, as indicated by the potential-dependent gravimetric capacitance obtained from cyclic voltammetry measurements (Fig. 2a). The typical gravimetric capacitance of LBL-MWNT electrodes in the voltage range 3–4.25 V versus Li (with a comparable voltage scale of 0 to ~1.2 V versus standard hydrogen electrode (SHE)) is ~125 F g^{-1}, which is comparable to the values reported for functionalized MWNTs[23,31] and porous carbon materials[32,33] in aqueous solutions. Reducing the lower potential limit from 3.0 to 1.5 V led to a significant increase in the gravimetric capacitance from ~125 to ~250 F g^{-1} measured at 4.0 and 2.5 V versus Li. Recent studies have shown that carbonyl (C=O) groups can be reduced by Li$^+$ and reversibly oxidized in the voltage range from ~3.5 to ~1.5 V versus Li in aromatic carbonyl derivative organic materials such as poly(2,5-dihydroxy-1,4-benzoquinone-3,6-methylene)[34] and Li$_2$C$_6$O$_6$ (ref. 35). It is therefore postulated
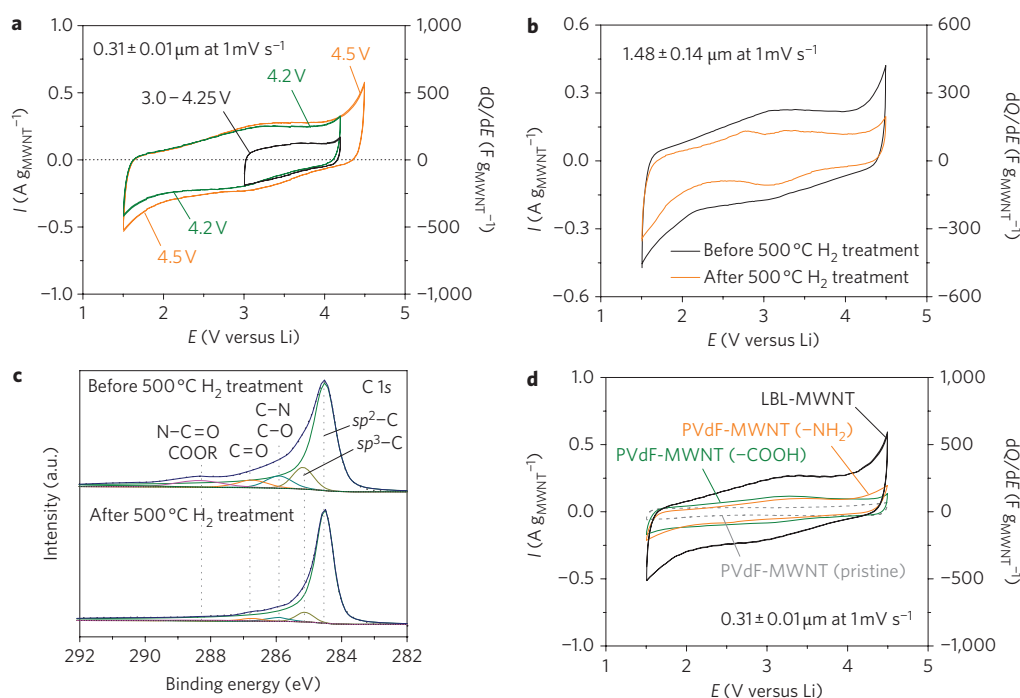
Figure 2 | Potential-dependent electrochemical behaviour of LBL-MWNT and functionalized MWNT composite electrodes measured in two-electrode lithium cells. a, Cyclic voltammogram data for an LBL-MWNT electrode obtained with different upper- and lower-potential limits. Reducing the lower-potential limit from 3 to 1.5 V versus Li resulted in increased current and gravimetric capacitance. **b**, Cyclic voltammogram data for an LBL-MWNT electrode before and after 500 °C H_2-treatment in 4% H_2 and 96% Ar by volume for 10 h. **c**, XPS C 1s spectra of an LBL-MWNT electrode before and after this additional heat treatment, which is seen to remove a considerable amount of surface oxygen and nitrogen functional groups from the MWNT surface. **d**, Cyclic voltammogram data for an LBL-MWNT electrode and composite electrodes of pristine MWNT, MWNT–COOH and MWNT–NH$_2$, with the LBL-MWNT electrode having higher current and capacitance normalized to the MWNT weight than the composite electrodes. The composite electrodes consisted of 20 wt% PVdF and 80 wt% MWNT. Composite MWNT electrodes were prepared from slurry casting and dried at 100 °C for 12 h under vacuum. The thickness of the LBL-MWNT electrode was 0.3 μm, and the thicknesses of the pristine MWNT, MWNT–COOH and MWNT–NH$_2$ composite electrodes were 40, 50 and 30 μm, respectively. The density of the composite electrodes was ~0.45 g cm^{-3}.

that the doubled gravimetric capacitance obtained from lowering the lower voltage limit of Li/LBL-MWNT cells (with open-circuit voltages of ~3.2 V) from 3.0 to 1.5 V versus Li can be attributed to the Faradaic reactions of surface oxygen on LBL-MWNTs, such as $C=O_{LBL\text{-}MWNT} + Li^+ + e^- \leftrightarrow C-OLi_{LBL\text{-}MWNT}$, which can become accessible at voltages lower than ~3 V versus Li.

The role of surface functional groups in providing high capacitances in LBL-MWNTs was further confirmed by comparing the specific capacitance of LBL-MWNTs before and after exposure to 4% H_2 and 96% Ar by volume at 500 °C for 10 h. The gravimetric current and capacitance values of the LBL-MWNT electrode decreased considerably (by 40%) after this heat treatment, as shown in Fig. 2b. XPS analysis showed that this high-temperature heat treatment decreased the amount of surface oxygen and nitrogen functional groups on the MWNTs. The intensities of the distinct C 1s peaks (assigned to carbon atoms in C−N (ref. 36) or C−O (ref. 37) centred at 285.9 ± 0.1 eV, carbonyl C=O (refs 27,37) groups at 286.7 ± 0.1 eV, and amide N−C=O or carboxylic COOR groups at 288.4 ± 0.1 eV (ref. 36)) were greatly reduced (by ~70%) relative to those of sp^2 (284.5 eV) and sp^3 (285.2 eV) hybridized carbon[37] following heat treatment, as shown in Fig. 2c. This experiment therefore provides further evidence that the redox of surface oxygen-containing functional groups with lithium ions is responsible for the large gravimetric capacitances of LBL-MWNT electrodes in organic electrolytes.

The contribution of double-layer capacitance to LBL-MWNT capacitances is relatively small compared to that of Faradaic reactions, and can be estimated by comparing cyclic voltammograms of composite electrodes (80 wt% MWNTs and 20 wt% binder) that include pristine MWNTs with those containing functionalized MWNTs

(see Supplementary Information). Composite electrodes with MWNT–COOH and MWNT–NH$_2$ show much higher gravimetric capacitances (factor of ~2) than pristine MWNTs (Fig. 2d; Supplementary Fig. S4), indicating the dominant contribution from the surface functional groups. In addition, we show that surface functional groups on MWNTs are better used in LBL-MWNT electrodes than in composite electrodes. The capacitance normalized to MWNT weight for LBL-MWNT electrodes is 2.5 times higher than that of conventional composite electrodes (Fig. 2d). Considering that the MWNT–COOH and MWNT–NH$_2$ in the composite electrodes have similar ratios of carbon and oxygen atomic percentages as the LBL electrodes (Supplementary Table S1), this result suggests that the binder-free porous network structure of LBL-MWNT electrodes allows better utilization of the surface functional groups than composite electrodes with binder, which can block the redox of the surface functional groups. Moreover, the volumetric capacitances of LBL-MWNT electrodes are even greater (by a factor of ~5) than those of composite MWNT electrodes because of their higher electrode density (0.83 g cm^{-3} for LBL-MWNTs versus 0.45 g cm^{-3} for composite electrodes).

Lithium storage characteristics of LBL-MWNT electrodes
The specific and volumetric capacitances of LBL-MWNT electrodes are greater than those of conventional composite electrodes based on carbon[32,38] in organic electrolytes. Because LBL-MWNT electrodes have no additives, the gravimetric capacitance normalized to electrode weight is identical to that normalized to MWNT weight. It is interesting to point out that the gravimetric capacitances of these LBL-MWNT electrodes are comparable to those of
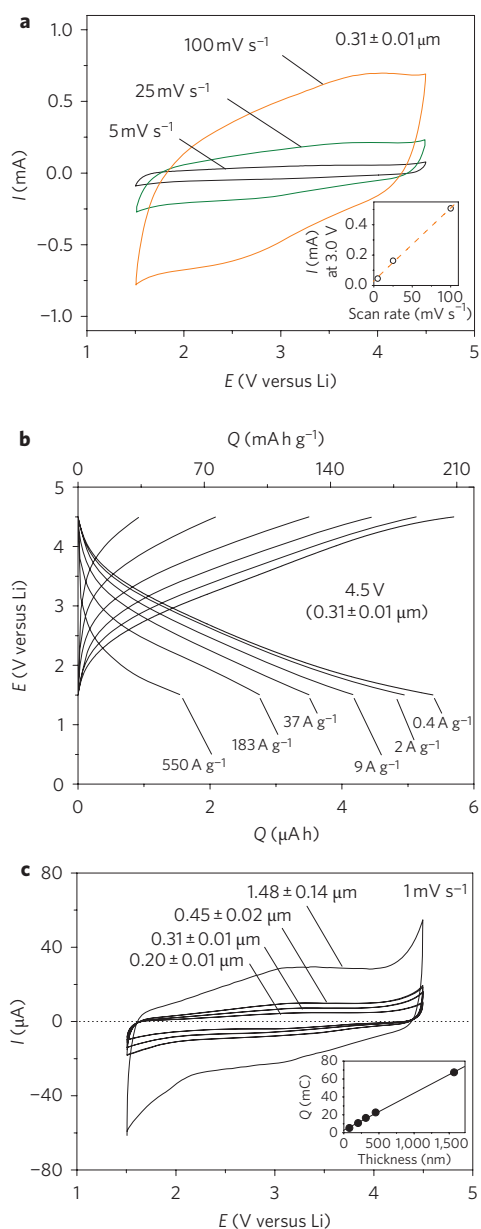
Figure 3 | Electrochemical characteristics of LBL-MWNT electrodes in two-electrode lithium cells with 1 M LiPF₆ in a mixture of ethylene carbonate and dimethyl carbonate (volume ratio 3:7). a, Cyclic voltammogram data for a 0.3-μm LBL-MWNT electrode over a range of scan rates. The current at ~3 V versus scan rate is shown in the inset. **b**, Charge and discharge profiles of an electrode of 0.3 μm obtained over a wide range of gravimetric current densities between 1.5 and 4.5 V versus Li. Before each charge and discharge measurement for the data in Fig. 3b, cells were held at 1.5 and 4.5 V for 30 min, respectively. **c**, Cyclic voltammogram data for electrodes with different thicknesses collected at a scanning rate of 1 mV s⁻¹ in the voltage range 1.5–4.5 V versus Li. The integrated charge increases linearly with electrode thickness, as shown in the inset.

nanostructured composite electrodes with manganese-based oxides (~40 wt% oxides), even though higher capacitances normalized to active material mass only (for example, up to ~600 F g_{MnO2}^{-1}; ref. 39) are typically reported. Moreover, taking into account the LBL-MWNT electrode density of 0.83 g cm⁻³, we obtain a volumetric capacitance of ~180 F cm⁻³ for LBL-MWNT electrodes, which is higher than that of nanostructured carbon (~50 F cm⁻³) in organic electrolytes[32] and nanostructured MnO₂ electrodes

(~150 F cm⁻³) in aqueous electrolytes[16,40]. Very few studies have reported the volumetric capacitance of entire electrodes, and we note that this is, to our knowledge, the highest value reported.

Storing energy on the surfaces of MWNTs enables LBL-MWNT electrodes to have a high rate capability. For a given thickness, the current at ~3 V was found to increase linearly with scan rate from cyclic voltammetry, indicating a surface-redox limited process (Fig. 3a, including inset), which is in good agreement with the proposed mechanism of redox of functional groups on MWNT surfaces. LBL-MWNT electrodes were also examined by means of galvanostatic measurements, allowing direct comparison with the performance of high-power battery materials. The gravimetric capacity of 0.3-μm electrodes was found to be ~200 mA h g⁻¹ at low rates such as 0.4 A g⁻¹, which is in good agreement with the estimated capacity of LBL-MWNT electrodes based on the proposed Faradaic reaction between Li and surface oxygen ($C_{0.86}O_{0.11}N_{0.04}$). Half of the gravimetric capacity (100 mA h g⁻¹) was retained at exceptionally high discharge rates of ~180 A g⁻¹ (corresponding to full discharge in less than 2 s), as shown in Fig. 3b. Moreover, the capacity (stored charge) of LBL-MWNT electrodes increases linearly with electrode thickness (Fig. 3c, inset), and a high power capability is maintained with electrode thickness increasing to 3 μm (Supplementary Fig. S5).

The specific energy and power of LBL-MWNT electrodes with thicknesses up to 3.0 μm, in the 1.5–4.5 V range, are shown in Fig. 4a (for volumetric energy and power data see Supplementary Fig. S7). Although the power capability of LBL-MWNT electrodes reduces somewhat with increasing thickness, electrodes of ~3.0 μm can still deliver a very high gravimetric energy of ~200 W h kg$_{electrode}^{-1}$ at a large gravimetric power of ~100 kW kg$_{electrode}^{-1}$, based on single-electrode weight alone. At low powers, their gravimetric energy (~500 W h kg$_{electrode}^{-1}$) approaches that of LiFePO₄ and LiCoO₂ (refs 5,35,41; Supplementary Fig. S6). At high powers (greater than 10 kW kg$_{electrode}^{-1}$), LBL-MWNT electrodes show higher gravimetric energy than carbon-nanotube-based electrodes for electrochemical capacitors (~70 W h kg$_{electrode}^{-1}$; ref. 25), thin-film batteries[22], nanostructured lithium battery materials[5,13] and high-power lithium battery materials[4,42] (Supplementary Fig. S6). As conventional composite electrodes are much thicker than the ~3.0-μm LBL-MWNT electrodes (>10 times), where ion transport in the electrodes can limit power capability, future studies are needed to examine how the power and energy performance of LBL-MWNT electrodes changes with thicknesses up to tens and hundreds of micrometres.

LBL-MWNT electrodes can be tested over 1,000 cycles without any observable capacity loss, as shown in Fig. 4b. Further cycling of a ~1.5-μm LBL-MWNT electrode revealed no capacity loss up to 2,500 cycles, even after the cell was left open circuit for 30 days (Supplementary Fig. S8). The voltage profiles in the first and 1,000th cycles to 4.5 V are virtually unchanged (Fig. 4c and Supplementary Fig. S8). TEM and XPS analysis of cycled electrodes (1,000 cycles to 4.5 V, followed by an additional 1,000 cycles to 4.7 V versus Li) provided further evidence for this cycling stability, with no distinctive change being noted in the surface atomic structure and surface functional groups after cycling (Supplementary Fig. S9). The stability of the functional groups on these MWNTs is remarkable when compared to the considerable losses of carbonyl derivative molecules within 50 to 100 cycles reported recently[34,35,43]. We hypothesize that the cycling stability of the LBL-MWNT electrodes can be linked to the strong chemical covalent bonding of the surface functional groups on the MWNTs, in contrast to the gradual separation occurring between the active carbonyl groups and carbon additives in composite electrodes during cycling.

Because a lithium negative electrode is not practical for real applications, we investigated the use of LBL-MWNT electrodes with a lithiated Li₄Ti₅O₁₂ (LTO) composite electrode (see
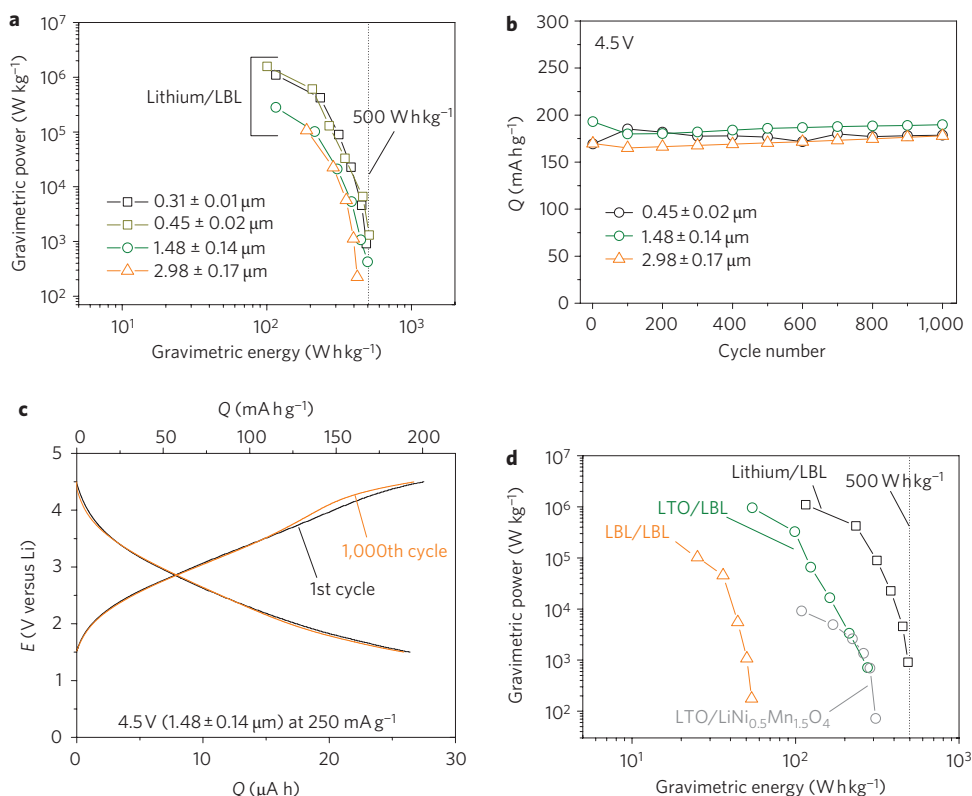
Figure 4 | Gravimetric energy and power densities, and cycle life of LBL-MWNT electrodes obtained from measurements of two-electrode cells. a, Ragone plot for Li/LBL-MWNT cells with different thicknesses (~0.3–3.0 μm). The corresponding loading density of LBL-MWNT electrodes ranges from ~0.025–0.25 mg cm^{-2}. Only the LBL-MWNT weight was considered in the gravimetric energy and power density calculations. **b**, Gravimetric capacities of Li/LBL-MWNT cells as a function of cycle number, measured at a current density of ~0.25 A g^{-1} once every 100 cycles, after voltage holds at the end of charging and discharging for 30 min. Within each 100 cycles, these cells were cycled at an accelerated rate of ~2.5 A g^{-1}. **c**, Voltage profiles of a 1.5-μm electrode in the first and 1,000th cycles, for which negligible changes were noted. **d**, Ragone plot for Li/LBL-MWNT (black squares), LTO/LBL-MWNT (green circles), LTO/LiNi$_{0.5}$Mn$_{1.5}$O$_4$ (grey circles) and LBL-MWNT/LBL-MWNT (orange triangles) cells with 4.5 V versus Li as the upper-potential limit. The thickness of the LBL-MWNT electrode was 0.3 μm for asymmetric Li/LBL-MWNT and LTO/LBL-MWNT, and 0.4 μm for symmetric LBL-MWNT/LBL-MWNT. Gravimetric energy and maximum power densities were reduced for the LTO/LBL-MWNT cells subjected to the same testing conditions due to a lower cell voltage.

Supplementary Information). Although the electrode gravimetric energy and power in LTO/LBL-MWNT cells is reduced due to the lower cell voltage (Fig. 4d), the rate capability, gravimetric capacity and capacity retention are comparable to cells with a Li negative electrode (Supplementary Fig. S10). Interestingly, although LTO/LBL-MWNT cells show comparable gravimetric energy to LTO/LiNi$_{0.5}$Mn$_{1.5}$O$_4$ cells at low power, they exhibit significantly higher gravimetric energy at powers greater than 10 kW kg$_{electrode}$$^{-1}$ (ref. 21; Fig. 4d and Supplementary Fig. S11). Using a conservative assumption that the mass of the battery is five times greater than that of the LBL-MWNT[22], which is higher than the 2.5 (ref. 4) typically used for conventional lithium rechargeable batteries due to reduced electrode thicknesses (such as 3 μm) demonstrated in this study, LTO/LBL-MWNT storage devices are expected to deliver ~30 W h kg$_{cell}$$^{-1}$ at ~5 kW kg$_{cell}$$^{-1}$. This value is significantly higher than that of current electrochemical capacitors with a gravimetric energy of ~5 W h kg$_{cell}$$^{-1}$ at ~1 kW kg$_{cell}$$^{-1}$ (refs 1,32).

Finally, we show that LBL-MWNT electrodes can also be used in symmetrical LBL-MWNT/LBL-MWNT cells (cell voltage in the range 0–3 V). As there is no net Faradaic reaction of surface oxygen-containing functional groups on MWNTs, they exhibit specific capacitances (~95 F g^{-1}) comparable to those (70 – 120 F g^{-1}) in electrochemical capacitors reported previously[44], but considerably lower than that of Li/LBL-MWNT cells. Symmetric cells therefore deliver gravimetric energy comparable to

conventional electrochemical capacitors[1,32], but lower than Li/LBL-MWNT and LTO/LBL-MWNT cells (Fig. 4d).

Conclusions
In summary, LBL-MWNT electrodes, which are conformal, densely packed and additive-free, can exhibit gravimetric energies up to ~200 W h kg$_{electrode}$$^{-1}$ at a gravimetric power of ~100 kW kg$_{electrode}$$^{-1}$, where the gravimetric energy and power at the cell level can be estimated by dividing these values by a factor of ~5. The energy stored in the LBL-MWNT electrodes can be controlled by the electrode thickness (Fig. 3c, inset) and upper voltage limit (Supplementary Fig. S12). Redox of surface oxygen-containing functional groups on LBL-MWNT electrodes by lithium ions in organic electrolytes, which can be accessed reversibly at high power, are predominantly responsible for the observed high energy and power capabilities of LBL-MWNT electrodes, as can be seen in the high-resolution TEM (HRTEM) image of the LBL-MWNT electrode in Fig. 5.

We have demonstrated energy and power capabilities of LBL-MWNT electrodes with thicknesses of a few micrometres that will open up new opportunities in the development of high-performance electrical energy storage for microsystems, and flexible, thin-film devices[22]. Further research will seek to validate the reported energy and power capabilities of MWNT electrodes with thicknesses of the order of tens and hundreds of micrometres, and minimize energy loss during charge and discharge (charging voltages of LBL-MWNT
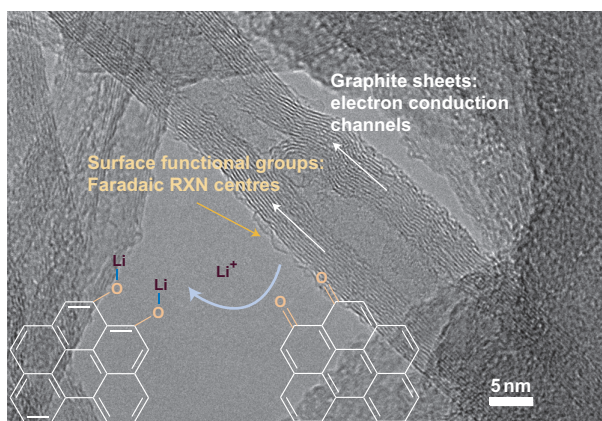
Figure 5 | Schematic of the energy storage mechanism of LBL-MWNT electrodes. Faradaic reactions between surface oxygen functional species (orange arrows) and Li schematically illustrated on an HRTEM image of the LBL-MWNT electrodes. Intact graphite layers inside the MWNTs (white arrows) are indicated as electron conduction channels.

electrodes are higher than those on discharge, even at low rates). Large-scale thicker electrodes of tens of micrometres can be produced using a recently developed sprayed LBL system[45] that uses an automated process to reduce assembly time dramatically (about 70 times faster than the conventional dipping of LBL systems used in this study). Modification of the surface functional groups on carbon[46,47] may allow the tuning of redox potentials and increase efficiency by reducing the voltage difference during charge and discharge.

Methods

Materials. MWNTs prepared by chemical vapour deposition were purchased from NANOLAB (95% purity; outer diameter, 15 ± 5 nm). Carboxylated MWNTs (MWNT–COOH) and amine-functionalized MWNTs (MWNT–NH$_2$) were prepared and assembled onto ITO-coated glass slides (procedures are described in detail elsewhere[23]). Cross-sectional scanning electron microscope (SEM) images of MWNT electrodes after heat treatments were obtained using a JEOL 6320 SEM operated at 5 kV.

Fabrication of layer-by-layer MWNT electrodes. MWNT–COOH and MWNT–NH$_2$ powder samples were sonicated for several hours in Milli-Q water (18 MΩ cm) to form a uniform dispersion, and this was followed by dialysis using Milli-Q water for several days, resulting in a stable dispersion of functionalized MWNTs in solution (0.5 mg ml^{-1}). pH values of the solutions were adjusted to pH 2.5 (MWNT–NH$_2$) and pH 3.5 (MWNT–COOH), respectively, and the solutions were sonicated for 1 h just before LBL assembly. All-MWNT electrodes were assembled with a modified Carl Zeiss DS50 programmable slide stainer. Details of LBL assembly of MWNT electrodes can be found elsewhere[23]. Assembled LBL-MWNT electrodes were dried in air, and these films were then heat-treated sequentially at 150 °C in vacuum for 12 h, and at 300 °C in H$_2$ for 2 h to increase mechanical stability.

X-ray photoelectron spectroscopy (XPS). A Kratos Axis Ultra XPS instrument (Kratos Analytical) with a monochromatized Al Kα X-ray source was used to analyse the surface chemistry of functionalized MWNTs and LBL-MWNT electrodes. The take-off angle relative to the sample substrate was 90°. Curve fitting of the photoemission spectra was performed following a Shirley-type background subtraction. An asymmetric C 1s peak from sp^2 hybridized carbons centred at 284.5 eV was generated for raw MWNTs. Using this asymmetric peak as a reference, all other peaks were fitted by the Gaussian–Lorentzian function. The experimental uncertainty of the XPS binding energy was ± 0.1 eV. The relative sensitivity factors used to scale the peaks of C 1s, O 1s and N 1s were 0.278, 0.780 and 0.477, respectively.

Electrochemical measurements. Electrochemical measurements were conducted using a two-electrode electrochemical cell (Tomcell) consisting of an LBL-MWNT electrode on ITO-coated glass, two sheets of microporous membrane (Celgard 2500, Celgard) and lithium foil as the counter-electrode. LBL-MWNT electrode areas of 100 or 50 mm^2 were used for electrochemical measurements with Li foil and lithiated LTO negative electrodes. The weights of the LBL-MWNT electrodes were determined from the area and the mass area density (see Supplementary Information). The loading density of the LBL-MWNT electrodes ranged from $\sim$0.025 to 0.25 mg cm^{-2}. A piece of aluminium foil (25 μm thick and with an area

of 1 mm × 7 mm in contact with the LBL-MWNT electrode) was attached to one edge and used as a current collector. The electrolyte solution was 1 M LiPF$_6$ dissolved in a mixture of ethylene carbonate (EC) and dimethyl carbonate (DMC) with a 3:7 volume ratio (3.5 ppm H$_2$O impurity, Kishida Chem.). The separators were wetted by a minimum amount of electrolyte to reduce the background current. Cyclic voltammetry and galvanostatic measurements of the lithium cells were performed using a Solartron 4170 at room temperature.

References

1. Simon, P. & Gogotsi, Y. Materials for electrochemical capacitors. *Nature Mater.* **7,** 845–854 (2008).
2. Miller, J. R. & Simon, P. Materials science—electrochemical capacitors for energy management. *Science* **321,** 651–652 (2008).
3. Amatucci, G. G., Badway, F., Du Pasquier, A. & Zheng, T. An asymmetric hybrid nonaqueous energy storage cell. *J. Electrochem. Soc.* **148,** A930–A939 (2001).
4. Kang, B. & Ceder, G. Battery materials for ultrafast charging and discharging. *Nature* **458,** 190–193 (2009).
5. Lee, Y. J. *et al.* Fabricating genetically engineered high-power lithium-ion batteries using multiple virus genes. *Science* **324,** 1051–1055 (2009).
6. Nazar, L. F. *et al.* Nanostructured materials for energy storage. *Int. J. Inorg. Mater.* **3,** 191–200 (2001).
7. Arico, A. S. *et al.* Nanostructured materials for advanced energy conversion and storage devices. *Nature Mater.* **4,** 366–377 (2005).
8. Poizot, P. *et al.* Nano-sized transition-metaloxides as negative-electrode materials for lithium-ion batteries. *Nature* **407,** 496–499 (2000).
9. Sides, C. R. *et al.* Nanoscale materials for lithium-ion batteries. *MRS Bull.* **27,** 604–607 (2002).
10. Bruce, P. G., Scrosati, B. & Tarascon, J. M. Nanomaterials for rechargeable lithium batteries. *Angew. Chem. Int. Ed.* **47,** 2930–2946 (2008).
11. Tarascon, J. M. & Armand, M. Issues and challenges facing rechargeable lithium batteries. *Nature* **414,** 359–367 (2001).
12. Armand, M. & Tarascon, J. M. Building better batteries. *Nature* **451,** 652–657 (2008).
13. Wu, X. L. *et al.* LiFePO$_4$ nanoparticles embedded in a nanoporous carbon matrix: superior cathode material for electrochemical energy-storage devices. *Adv. Mater.* **21,** 2710–2714 (2009).
14. Chmiola, J. *et al.* Anomalous increase in carbon capacitance at pore sizes less than 1 nanometer. *Science* **313,** 1760–1763 (2006).
15. Hu, C. C., Chen, W. C. & Chang, K. H. How to achieve maximum utilization of hydrous ruthenium oxide for supercapacitors. *J. Electrochem. Soc.* **151,** A281–A290 (2004).
16. Fischer, A. E. *et al.* Incorporation of homogeneous, nanoscale MnO$_2$ within ultraporous carbon structures via self-limiting electroless deposition: implications for electrochemical capacitors. *Nano Lett.* **7,** 281–286 (2007).
17. Reddy, A. L. M., Shaijumon, M. M., Gowda, S. R. & Ajayan, P. M. Coaxial MnO$_2$/carbon nanotube array electrodes for high-performance lithium batteries. *Nano Lett.* **9,** 1002–1006 (2009).
18. Kim, D. K. *et al.* Spinel LiMn$_2$O$_4$ nanorods as lithium ion battery cathodes. *Nano Lett.* **8,** 3948–3952 (2008).
19. Bélanger, D., Brousse, T. & Long, J. W. Manganese oxides: battery materials make the leap to electrochemical capacitors. *Electrochem. Soc. Interf.* **17,** 49–52 (2008).
20. Decher, G. Fuzzy nanoassemblies: toward layered polymeric multicomposites. *Science* **277,** 1232–1237 (1997).
21. Xiang, H. F. *et al.* Effect of capacity matchup in the LiNi$_{0.5}$Mn$_{1.5}$O$_4$/Li$_4$Ti$_5$O$_{12}$ cells. *J. Power Sources* **183,** 355–360 (2008).
22. Dudney, J. N. Thin film micro-batteries. *Electrochem. Soc. Interf.* **17,** 44–48 (2008).
23. Lee, Seung Woo *et al.* Layer-by-layer assembly of all carbon nanotube ultrathin films for electrochemical applications. *J. Am. Chem. Soc.* **131,** 671–679 (2009).
24. Niu, C. M. *et al.* High power electrochemical capacitors based on carbon nanotube electrodes. *Appl. Phys. Lett.* **70,** 1480–1482 (1997).
25. Futaba, D. N. *et al.* Shape-engineerable and highly densely packed single-walled carbon nanotubes and their application as super-capacitor electrodes. *Nature Mater.* **5,** 987–994 (2006).
26. Zielke, U., Huttinger, K. J. & Hoffman, W. P. Surface-oxidized carbon fibers: I. Surface structure and chemistry. *Carbon* **34,** 983–998 (1996).
27. Kozlowski, C. & Sherwood, P. M. A. X-ray photoelectron-spectroscopic studies of carbon-fibre surfaces. Part 5. The effect of pH on surface oxidation. *J. Chem. Soc. Farad. Trans. I* **81,** 2745–2756 (1985).
28. Frackowiak, E. *et al.* Electrochemical storage of lithium multiwalled carbon nanotubes. *Carbon* **37,** 61–69 (1999).
29. Zhu, X. Y., Lee, S. M., Lee, Y. H. & Frauenheim, T. Adsorption and desorption of an O$_2$ molecule on carbon nanotubes. *Phys. Rev. Lett.* **85,** 2757–2760 (2000).
30. Burg, P. *et al.* The characterization of nitrogen-enriched activated carbons by IR, XPS and LSER methods. *Carbon* **40,** 1521–1531 (2002).

31. Lota, G. *et al.* Effect of nitrogen in carbon electrodes on the supercapacitor performance. *Chem. Phys. Lett.* **404,** 53–58 (2005).

32. Simon, P. & Burke, A. Nanostructured carbons: double-layer capacitance and more. *Electrochem. Soc. Interf.* **17,** 38–43 (2008).

33. Chmiola, J., Yushin, G., Dash, R. & Gogotsi, Y. Effect of pore size and surface area of carbide derived carbons on specific capacitance. *J. Power Sources* **158,** 765–772 (2006).

34. Le Gall, T., Reiman, K. H., Grossel, M. C. & Owen, J. R. Poly(2,5-dihydroxy-1,4-benzoquinone-3,6-methylene): a new organic polymer as positive electrode material for rechargeable lithium batteries. *J. Power Sources* **119,** 316–320 (2003).

35. Chen, H. *et al.* From biomass to a renewable $Li_xC_6O_6$ organic electrode for sustainable Li-ion batteries. *ChemSusChem* **1,** 348–355 (2008).

36. Ramanathan, T., Fisher, F. T., Ruoff, R. S. & Brinson, L. C. Amino-functionalized carbon nanotubes for binding to polymers and biological systems. *Chem. Mater.* **17,** 1290–1295 (2005).

37. Ago, H. *et al.* Work functions and surface functional groups of multiwall carbon nanotubes. *J. Phys. Chem. B* **103,** 8116–8121 (1999).

38. Naoi, K. & Simon, P. New materials and new configurations for advanced electrochemical capacitors. *Electrochem. Soc. Interf.* **17,** 34–37 (2008).

39. Ma, S. B. *et al.* Electrochemical properties of manganese oxide coated onto carbon nanotubes for energy-storage applications. *J. Power Sources* **178,** 483–489 (2008).

40. Fischer, A. E. *et al.* Electroless deposition of nanoscale MnO_2 on ultraporous carbon nanoarchitectures: correlation of evolving pore–solid structure and electrochemical performance. *J. Electrochem. Soc.* **155,** A246–A252 (2008).

41. Whittingham, M. S. Lithium batteries and cathode materials. *Chem. Rev.* **104,** 4271–4301 (2004).

42. Kang, K. S. *et al.* Electrodes with high power and high capacity for rechargeable lithium batteries. *Science* **311,** 977–980 (2006).

43. Chen, H. Y. *et al.* Lithium salt of tetrahydroxybenzoquinone: toward the development of a sustainable Li-ion battery. *J. Am. Chem. Soc.* **131,** 8984–8988 (2009).

44. Frackowiak, E. & Beguin, F. Carbon materials for the electrochemical storage of energy in capacitors. *Carbon* **39,** 937–950 (2001).

45. Krogman, K. C., Zacharia, N. S., Schroeder, S. & Hammond, P. T. Automated process for improved uniformity and versatility of layer-by-layer deposition. *Langmuir* **23,** 3137–3141 (2007).

46. Han, X. Y. *et al.* Aromatic carbonyl derivative polymers as high-performance Li-ion storage materials. *Adv. Mater.* **19,** 1616–1621 (2007).

47. Xiang, J. F. *et al.* A novel coordination polymer as positive electrode material for lithium ion battery. *Cryst. Growth Des.* **8,** 280–282 (2008).

Author contributions

Y.S.H., S.W.L., N.Y. and B.M.G. conceived and designed the experiments. S.W.L., B.S.K. and P.T.H. were involved with the methods of film assembly. S.C. carried out microscopy analysis. Y.S.H., S.W.L., N.Y. and B.M.G. co-wrote the manuscript, and P.T.H. edited the manuscript.

Additional information

The authors declare no competing financial interests. Supplementary information accompanies this paper at www.nature.com/naturenanotechnology. Reprints and permission information is available online at http://npg.nature.com/reprintsandpermissions/. Correspondence and requests for materials should be addressed to Y.S.H.